JOURNAL OF THE ROYAL SOCIETY Interface

J. R. Soc. Interface (2012) **9**, 389–395
doi:10.1098/rsif.2011.0671
Published online 23 November 2011

Report

Bioinspired bubble design for particle generation

Oguzhan Gunduz[1,2], Zeeshan Ahmad[3,*], Eleanor Stride[1], Candan Tamerler[4] and Mohan Edirisinghe[1]

[1]*Department of Mechanical Engineering, University College London, Torrington Place, London WC1E 7JE, UK*
[2]*Department of Metal Education, Technical Education Faculty, Marmara University, Istanbul 34722, Turkey*
[3]*School of Pharmacy and Biomedical Sciences, University of Portsmouth, Saint Michaels Building, White Swan Road, Portsmouth PO1 2DT, UK*
[4]*Materials Science and Engineering, University of Washington, Seattle, WA 98195, USA*

In this study, we devise a method to generate homogeneous particles from a bubble suspension, with the capability to control loading and the structure of bubbles. Ideally, a process such as this would occur at the interface between daughter bubble formation (instant) and gaseous diffusion (gradual). Interestingly, the budding mechanism in micro-organisms is one that demonstrates features of the desired phenomena (although at a much slower rate), as viruses can eject and evolve structures from their membranes. With these natural concepts, a bubble's surface can also be made to serve as a platform for particle generation, which transfers significant elements from the initial bubble coating to the newly generated structures. Here, we illustrate this by preparing coated bubbles (approx. 150 μm in diameter) using a hydrophobic polymer, which may be comparable to naturally occurring bubble coatings (e.g. organic matter forming part of bubble coatings in the sea), and dye (which can demonstrate entrapment of smaller quantities of a desired moiety) and then observe particle generation (approx. 500 nm). The process, which may be driven by a polymerosome-forming mechanism, also illustrates how additional uniform sub-micrometre-scale structures may form from a bubble's surface, which may have also previously been attributed to gas diffusion. In addition, such methods of particle formation from a bubble structure, the incorporation of chemical or biological media via an *in situ* process and subsequent release technologies have several areas of interest across the broad scientific community.

Keywords: bubble; bioinspired; particle; homogeneous; polymerosome; rippling

1. INTRODUCTION

The importance of bubbles in recent times is being 'blown' to new horizons, with their promising roles crossing physical and life sciences. Today, they are finding applications and implications in numerous areas of daily interactions spanning several disciplines, including engineering, environmental, food and healthcare sciences [1–3]. Often overlooked and seen as being of little significance, bubbles also occur naturally in several environments such as oceans and volcanoes [4,5]. In some of these domains, naturally occurring organic matter coats these bubble structures and, as a result of gaseous diffusion, particulate matter is formed [6]. In other instances, when these structures collapse, they form daughter bubbles, which are, again, significantly smaller in size but greater in number [7]. With such processes, there is a natural scaling down in size, which can also lead to an increase in the number of resulting structures. Inspired by such natural phenomena (figure 1) and also interesting structural changes during several bioprocesses (e.g. the budding mechanism in micro-organisms, where structures are formed from membranes with essential biological data intact [8,9]), it is possible to develop a bubble system that incorporates key elements from these various mechanisms, ideally leading to the development of a versatile and modular approach to preparing a novel bubble system that generates active homogeneous particles by controlling polymer behaviour in appropriate environments (e.g. polymerosomes) [10]. The resulting particles can also be made to integrate components of the initial bubble coating, which can be varied

*Author for correspondence (zeeshan.ahmad@port.ac.uk).

Electronic supplementary material is available at http://dx.doi.org/10.1098/rsif.2011.0671 or via http://rsif.royalsocietypublishing.org.

Received 2 October 2011
Accepted 3 November 2011

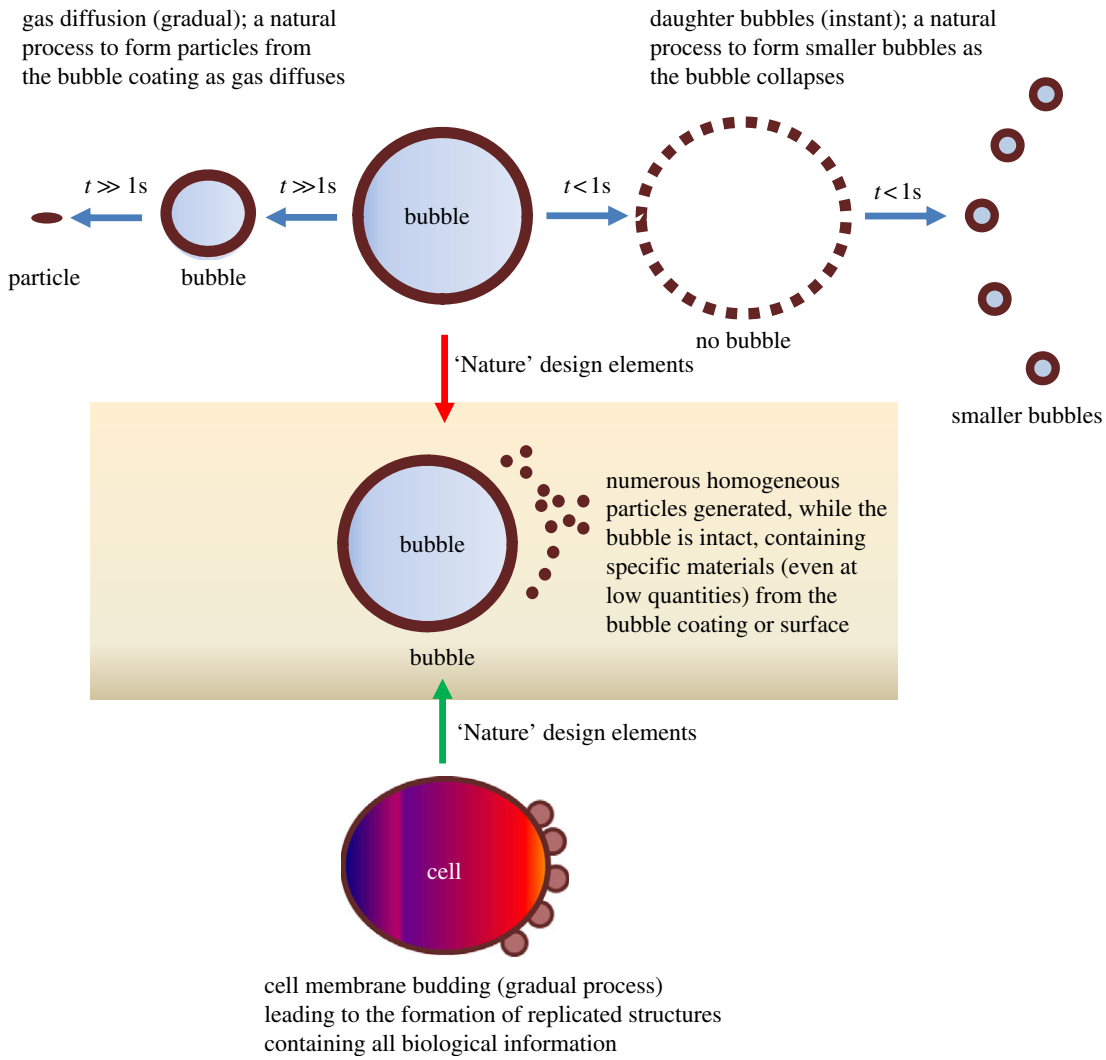

Figure 1. Nature and bioinspired bubble design elements.

to contain a host of chemicals and biologically significant agents [11,12].

Bubbles are critically important in diagnostics and especially in targeted therapeutics. Advances in physical and engineering sciences have provided novelties in the composition of bubble structures, such that they can have patterned surfaces [13] and multi-layered coatings [14] or have armoured non-spherical shapes [15]. However, for the release of agents from such structures, most, if not all, developmental effort has been focused on instant bubble breakdown to deliver a desired therapeutic effect, and the challenges to develop smart bubble systems that complement, compete with or replace traditional methods (e.g. encapsulated particles) remain. Naturally occurring bubbles also exhibit certain characteristics, owing largely to their local environs, which dictate not only the composition of such structures but also how they break down. The use of high-speed imaging and modelling has recently elucidated complex mechanisms in such processes that are not visible to the naked eye [7]. Because of this, the common concept of a 'bubble', which is viewed as encapsulating air by a very thin material [16] that then 'vanishes' after it collapses, also needs to be revisited as there are several processes that can occur in dictating how a bubble will collapse and/or result in controlled formation of matter. Some of these have been seen to occur naturally, e.g. particle formation due to gas exchange, which is the cause of some particle formation in oceans and rivers (over a prolonged time period), or daughter bubble formation (directly from collapsing bubbles).

As the application potential of bubbles has increased and diversified into those requiring greater technical specification, so too have the various methods of generating bubbles [17]. In such methods, the polydispersivity of bubbles is often compromised and can result in a bimodal distribution [18,19]. Simple microfluidic models enable greater control of the size range of bubbles in sample sets, thus reducing any possible deviations based on bubble size variations. In the preparation of bioinspired particles from a bubble structure, a simple microfluidic device was used to demonstrate the principles that could be adapted to other methods of bubble generation.

2. MATERIAL AND METHODS

2.1. Materials

Polymethylsilsesquioxane (PMSQ) was purchased from Wacker-Chemie, GmbH (Burghausen, Germany; density,

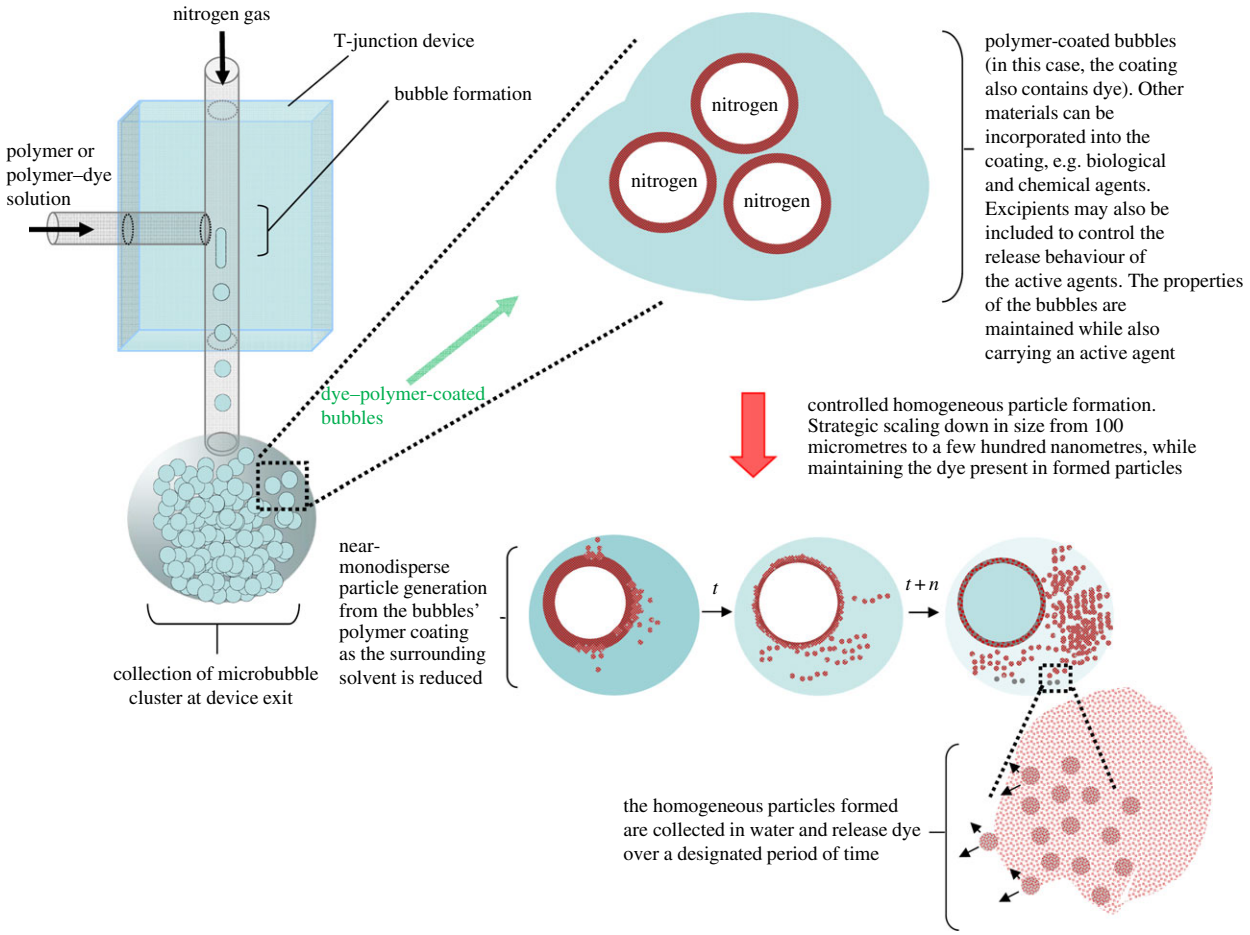

Figure 2. Bubble preparation using a T-junction microfluidic device. These can be made to contain polymer (PMSQ) or polymer–dye (PMSQ–haematoxylin) compositions. Bubbles (approx. 150 μm in diameter) were collected at the exit of the device. Resulting (approx. 500 nm) particles comprised polymeric media from the bubbles' coating.

1240 kg m^{-3}; molecular weight, 9600 g mol^{-1}). Ethanol was purchased from VWR International Ltd (purity grade, 99.7–100%; density, 790 kg m^{-1}). Haematoxylin dye was purchased from Sigma-Aldrich (Poole, UK) and was used in this study as a model release agent. Nitrogen gas was supplied by BOC, UK.

2.2. Methods

The surface tension of the 40 wt% PMSQ–ethanol solution was measured using a Krüss tensiometer.

The microfluidic T-junction device was manufactured in Turkey (Gunay-Yag Co.) and was used to demonstrate 'particle-generating bubbles' or 'active particle-generating bubbles' (PGBs or APGBs, respectively). The tubing in the T-junction device was constant for all inlets (inner diameter, 150 μm; outer diameter, 1590 μm). Using this device PGBs/APGBs were generated by accommodating the flow of two separate phase media—a gas (nitrogen) and a selected polymer solution (PMSQ with and without haematoxylin dye). Such microfluidic devices provide significant control over the polydispersitivity and bubble size; however, the size is dependent on the diameter of the capillary tubing used to form the bubbles [20].

For imaging, a Nikon Eclipse ME-600 optical microscope, JEOL JSM-6301F electron microscope and Phantom V7 high-speed camera were used. With optical and high-speed imaging, the various stages of the PGBs' lifetime were observed, delivering predictable control of the structures. The dispersed dye–polymer particles (serving here as the 'active' particles) formed from the bubble carrier system demonstrated controlled release, exhibiting the potential impact in life science remits. To assess the release of dye from generated particles, samples were centrifuged at 3313g for 30 min. The supernatant was removed and its absorbance was measured using a UV spectrometer (Lambda 35, Perkin Elmer, UK).

A schematic detailing this and the experimental methodology is shown in figure 2.

3. RESULTS AND DISCUSSION

Conventionally, bubbles are generated at the gas–liquid interface at the various channel or capillary intersections [18], and there are advanced laboratory-chip devices or manifolds that have multiple junctions and flows, all of which use this underlying principle. The simplistic two-inlet device used here (figure 3*a*) generated bubbles at a single perpendicular junction (figure 3*b*), and the resultant bubble clusters were collected at the device exit (figure 3*c*). The flow of gas was supplied by a pressurized cylinder (with a controllable pressure gauge) and the polymeric media (optimal at 40 wt% in ethanol with

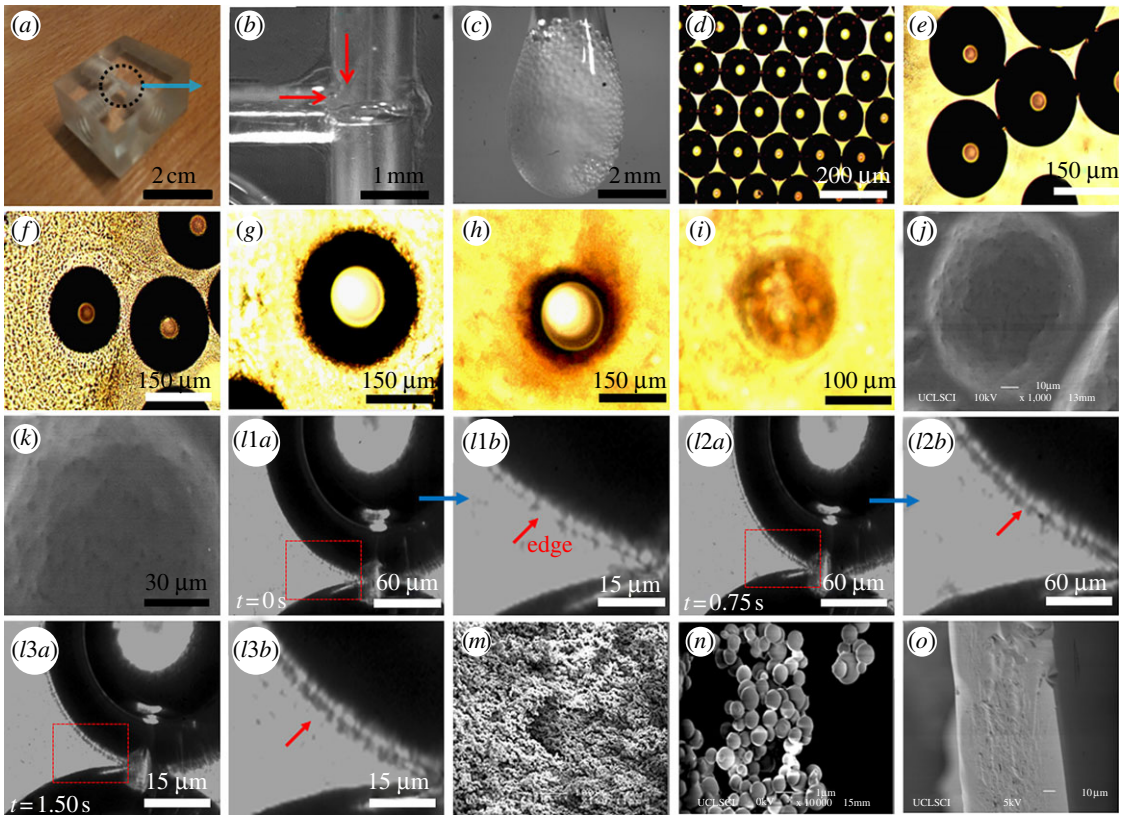

Figure 3. Structures observed during various steps of experiments. (*a*) The microfluidic device used in this study; (*b*) high-speed image of bubble flow through the microfluidic channel directly after formation; (*c*) high-speed image showing the collection of bubble (individual bubbles approx. 150 µm) clusters (1500 µm) at the device exit. Optical micrographs of bubbles at a post-collection time of (*d*) approximately 30 s at low magnification, (*e*) 30 s with reduced backlight, (*f*) approximately 60 s, when particle generation is clearly evident. (*g*) A close-up micrograph of particle generation at approximately 120 s and (*h*) changes to the bubble surface as particle generation continues; with a corona of particles visible on its surface until (*i*) the bubble collapses and a template of the bubble remains after the majority of the surface is reduced after particle generation. (*j*) A scanning electron micrograph showing frozen bubbles (immersed in liquid nitrogen) at $t = 80$ s and (*k*) a close-up micrograph showing protruding sites on the frozen surface. (*l*1*a*–*l*3*b*) Activity at the bubbles' surface observed over a period of 2 s using a high-speed camera at different time intervals and magnifications during particle generation. Resultant particles from polymeric bubbles are shown in (*m*) low magnification and (*n*) high magnification, with an excellent monodisperse size of approximately 500 nm. Without the use of any bubbles, there is a distinct difference in the outcome of solvent drying in a 40 wt% PMSQ solution, as shown in panel (*o*), demonstrating a non-particle film morphology.

addition of haematoxylin dye ($\lambda = 356$ nm) for selected experiments) were infused using a precision pump. Under optimal conditions (gas flow, 140–180 kPa; polymer solution flow, 700–800 µl min^{-1}), near-monodisperse bubbles were generated. Bubbles were approximately 150 µm in diameter when collected on a glass slide and observed under an optical microscope at a post-collection time of approximately 30 s (figure 3*d*,*e*, reduced backlight). At this time, point bubbles remain stable and are indicative of typical structures produced in earlier studies using microfluidic devices, displaying an ordered layering [20]. However, after a time interval of approximately 60 s particle generation becomes evident (figure 3*f*); this becomes vigorous and dynamic after a time interval of approximately 120 s (figure 3*g*), when the polymer coating on the bubbles resembles a pulsating halo. Particles continue to be generated and the initial polymer coating is significantly changed (figure 3*h*). The bubble then finally collapses, leaving a template of the bubbles at the final location (figure 3*i*).

The underlying mechanism of PGBs/APGBs depends on the nature of the polymer, its solubility in the selected solvent and the rate at which this solvent evaporates. The polymer displays partial solubility in ethanol and is insoluble in water [21] and the polymer solution has a low surface tension (24 mN m^{-1}), which favours the initial bubble formation from the microfluidic device. Previous studies have demonstrated the formation of particles from polymeric droplets in double-emulsion systems (polymerosomes), which is driven by a self-assembly mechanism during solvent evaporation [10]. During the initial stages of the bubble life cycle, there may be polymer dissolution from the surface of the bubbles into the ethanol solution, which may also contribute towards the generation of particles during solvent evaporation. However, as the solvent is volatile, the particle-generating process becomes more concentrated near the bubbles' surface and is accelerated towards the end of the bubbles' lifespan (prior to collapsing; electronic supplementary material, supplementary videos S1 and S2). During this stage, the polymer content in the coating increases from the initial 40 wt% and surpasses the critical concentration required to enable precipitation and assembly of particles, which may also be favourable owing to the partial solubility of PMSQ in

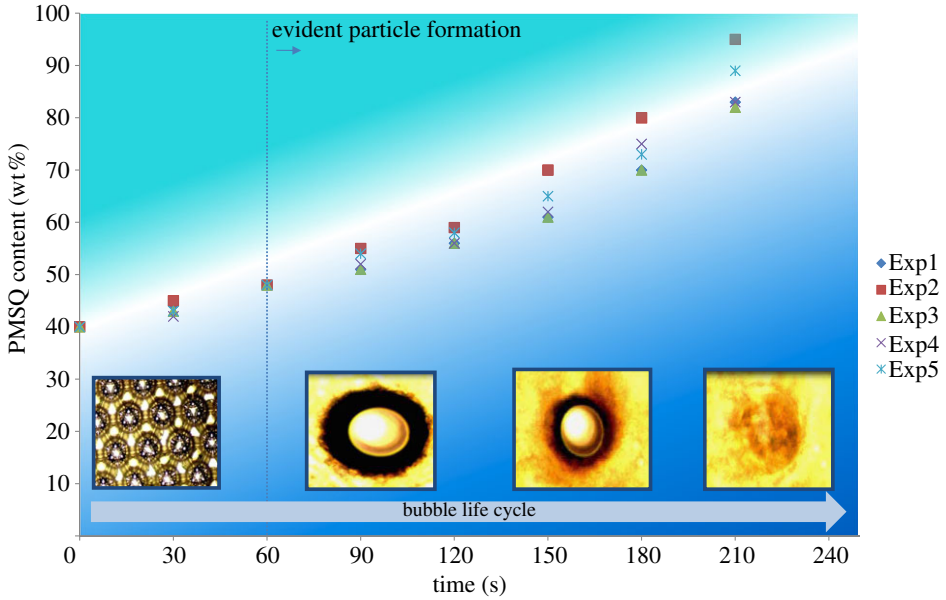

Figure 4. Bubble and structural evolution due to solvent evaporation (and therefore resulting polymer concentration) at selected time intervals. Various bubble samples based on collection time: Exp1, 2 s; Exp2, 4 s; Exp3, 6 s; Exp4, 8 s; and Exp5, 10 s.

ethanol. Electron microscopy of bubble structures during the particle-generating stages (by immersing bubbles in liquid nitrogen after a time interval of approx. 80 s post collection) reveals the bubble coating structure (figure 3*j*) and retains the micrometre- and sub-micrometre-sized protrusions from where polymeric particles may have originated (figure 3*k*).

Observing the behaviour of APGBs/PGBs under an optical microscope demonstrates various stages of particle generation over broad time intervals, which may be too rapid to observe significant changes at or close to the APGB/PGB surface. APGBs/PGBs can also be visualized over reduced time scales using a high-speed camera, which gives a better indication of the rate at which particles may evolve in this process. Figure 3*l*1*a*–3*l*3*b* shows a PGB over a time period of 2 s during particle generation. There is very little noticeable difference between consecutive frames (approx. 6000 frames per second) during high-speed imaging, and three time points were selected to demonstrate the distinct changes on the surface of the APGB/PGB. There is a clear difference in structures between time periods of 0 s (figure 3*l*1*a*,*b*), 0.75 s (figure 3*l*2*a*,*b*) and 1.50 s (figure 3*l*3*a*,*b*), with a gradual increase in particles on the surface over the time period. The particles produced were approximately 500 nm, as shown in a cross section of a dried agglomerate structure obtained 24 h post collection (figure 3*m*), were perfectly spherical and also had a near-monodisperse size distribution. On closer (figure 3*n*) inspection, these are also comparable to the protrusion size observed for the APGB/PGB samples captured using liquid nitrogen.

Depositing the same polymeric solution (used for bubble preparation) on a glass slide, without the presence of any bubbles, results in film formation without any particulate morphology, which is evident from a cross section and surface analysis of the resulting structure (figure 3*o*). The disparity in these structures can be attributed to the role of polymeric bubbles in controlled particle formation. The inner gaseous component of the bubble is encapsulated by the polymer. The outer side of the polymer coating is exposed to a partially soluble solvent that is evaporating at a rapid rate. With this interface the diffusion is controlled, as the polymer can only form and disperse in the direction of the evaporating solvent. As the solvent content reduces and reaches a critical value, homogeneous polymeric particles are formed owing to precipitation. The particles formed will not merge to form any secondary structures as the solvent concentration is significantly reduced and so will not have any dissolution effect. In contrast, this is not the case with a drying polymeric droplet, which will undergo solvent evaporation and polymer precipitation with very little control throughout the structure. The rate at which solvent evaporation occurs can be monitored by measuring the mass loss from a series of bubble samples (on a sealed edge glass slide) that enable critical polymer concentrations to be determined at the various bubble stages during the particle-generating process; these time points are highlighted in figure 4. At a post-collection time of 60 s (when particle formation is evident), the corresponding mass composition of polymer in the system is closer to approximately 47 per cent, which signifies a 7 per cent increase from the concentration used as the initial bubble coating. This particle-generating process becomes more prominent as a function of time and solvent evaporation (and as a function of an increase in polymer concentration). A time interval of approximately 210 s corresponds to polymer concentrations between 80 and 93 per cent, which is more than a twofold increase in the starting concentration; by this stage, the bubble has already collapsed. However, from our observations, bubbles can remain intact when the polymer concentration reaches up to 76 per cent during the particle-generating process.

Although the polymer concentration increases owing to solvent evaporation, there is continued loss of polymer from the surface of the bubbles as a result of particle generation from the precipitation process. In

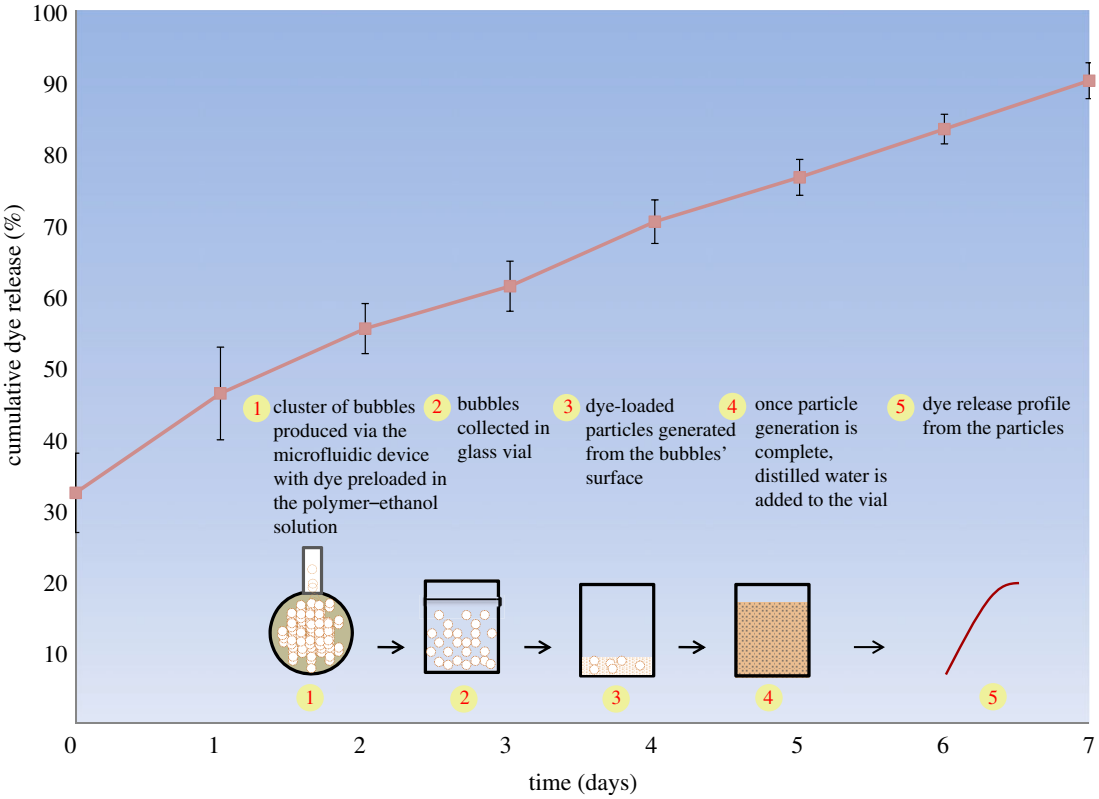

Figure 5. Dye release profiles using a pre-loaded dye–polymer solution to generate bubbles and subsequent particle generation. The release profile is over a seven-day period.

addition to this, the bubble surface is also changing physically, which causes deformations very similar to the rippling effect associated with bubbles [22]. This effect becomes more evident closer to the end of the APGB/PGB life cycle.

The proposed APGBs/PGBs provide a method for scaling down structures *in situ*. For example, the initial micrometre-sized bubble structures generate uniform sub-micrometre-sized particles, from a single structure, with a size difference of over two orders of magnitude. In addition to previous examples (gas diffusion and the formation of a ring of miniaturized daughter bubbles), this mechanism contributes towards the various ways in which bubbles collapse or break down. PGBs may already exist as various organic materials contribute towards bubble coatings (e.g. at sea water interfaces [23]) which may subsequently be subjected to drying, albeit it at a significantly reduced rate. However, as is the case with the forming of daughter bubbles, the conditions for APGBs/PGBs must be correct.

APGBs/PGBs may also play a role in particle formation, which may have previously been overlooked and possibly attributed to different mechanisms. The encapsulating ability of the coating material(s) may serve as an indicator of the origins of particles that may have formed from such processes. Alternatively, as APGBs may also be used as novel devices for *in situ* formation and encapsulation, these may have applications in several branches of science. To demonstrate this, a small quantity of haematoxylin (dye) was added to the polymeric solution prior to bubble formation.

Figure 5 shows the release profiles and methodology followed during this process. In the preparation of APGBs (with and without dye), there was no significant difference in bubble size and particles formed during the process. Both polymeric and polymer–dye systems displayed similar bubble (approx. 150 µm) and generated particle (approx. 500 nm) size, and these were collected in water at a post-collection time of 200 s. Dye was trapped inside the generated particles. The release profile demonstrated a diffusion-based release mechanism, resulting in zero-order elimination of dye from the resultant particles. Therefore, using this particle-forming method, the origin of a PGB/APGB may be traced if residual chemical moieties remain trapped within particles after they have been generated.

4. CONCLUDING REMARKS

APGBs/PGBs offer an innovative and comparative approach to encapsulating desirable chemical and biological compounds into homogeneous micrometre- and sub-micrometre-sized structures *in situ*, which has been likened to a rapid adaptation of the budding process in viruses, where identical structures (which also contain crucial chemical or biological molecules) are formed from the organism's membrane. For example, when compared with conventional layered structures comprising two or more materials (non-active outer layer surrounding an active inner layer), APGBs form and release smaller structures from the same coarse carrier (under the appropriate conditions). Furthermore, such structures can also be used to detect or locate matter that has been demonstrated previously with bubbles using different methods. This work also shows that dispersed

particles can be generated from bubbles in large quantities, without the collapse of bubbles, and may also contribute towards particle formation in everyday instances from lakes to cooking environments where bubbles may be formed by routine and natural processes. The underlying process may be attributed to polymerosome-forming mechanisms, but is seen to be more favourable in this instance with a bubble system, which is desirable as the emerging benefits of bubbles (use as contrast agents and ultrasound trigger response) can be readily adapted to such systems.

The authors thank the Islamic Development Bank (IDB) and the Merit Scholarship Programme for High Technology (MSP) for funding O.G.'s PhD research at UCL. They also acknowledge Adrian Walker and the EPSRC for loaning their high-speed camera.

REFERENCES

1 Shang, J., Chen, B., Lin, W., Wong, C. P., Zhang, D., Xu, C., Junwen, L. & Huang, Q. A. 2011 Preparation of wafer-level glass cavities by a low-cost chemical foaming process (CFP). *Lab Chip* **11**, 1532–1540. (doi:10.1039/C0LC00708K)
2 Stramski, D., Boss, E., Bogucki, D. & Voss, K. J. 2004 The role of seawater constituents in light backscattering in the ocean. *Prog. Oceanogr.* **61**, 27–56. (doi:10.1016/j.pocean.2004.07.001)
3 Chiu, S. H. & Liu, C. H. 2009 An air-bubble-actuated micropump for on-chip blood transportation. *Lab Chip* **9**, 1524–1533. (doi:10.1039/B900139E)
4 Deane, G. B. & Stokes, M. D. 2002 Scale dependence of bubble creation mechanisms in breaking waves. *Nature* **418**, 839–844. (doi:10.1038/nature00967)
5 Woods, A. W. & Cardoso, S. S. S. 1997 Triggering basaltic volcanic eruptions by bubble-melt separation. *Nature* **385**, 518–520. (doi:10.1038/385518a0)
6 Johnson, B. D. 1976 Nonliving organic particle formation from bubble dissolution. *Limnol. Oceanogr.* **21**, 444–446. (doi:10.4319/lo.1976.21.3.0444)
7 Bird, J. C., de Ruiter, R., Courbin, L. & Stone, H. A. 2010 Daughter bubble cascades produced by folding of ruptured thin films. *Nature* **465**, 759–762. (doi:10.1038/nature09069)
8 Hurley, J. H., Boura, E., Carlson, L. A. & Rozycki, B. 2010 Membrane budding. *Cell* **143**, 875–887. (doi:10.1016/j.cell.2010.11.030)
9 Raiborg, C. & Stenmark, H. 2009 The ESCRT machinery in endosomal sorting of ubiquitylated membrane proteins. *Nature* **458**, 445–452. (doi:10.1038/nature07961)
10 Lorenceau, E., Utada, A. S., Link, D. R., Cristobal, G., Joanicot, M. & Weitz, D. A. 2005 Generation of polymerosomes from double-emulsions. *Langmuir* **21**, 9183–9186. (doi:10.1021/la050797d)
11 Huang, S. L., McPherson, D. B. & MacDonald, R. C. 2008 A method to co-encapsulate gas and drugs in liposomes for ultrasound-controlled drug delivery. *Ultrasound Med. Biol.* **34**, 1272–1280. (doi:10.1016/j.ultrasmedbio.2008.01.005)
12 Castro-Hernandez, E., van Hoeve, W., Lohse, D. & Gordillo, J. M. 2011 Microbubble generation in a co-flow device operated in a new regime. *Lab Chip* **11**, 2023–2029. (doi:10.1039/C0LC00731E)
13 Dressaire, E., Bee, R., Bell, D. C., Lips, A. & Stone, H. A. 2008 Interfacial polygonal nanopatterning of stable microbubbles. *Science* **320**, 1198–1201. (doi:10.1126/science.1154601)
14 Ahmad, Z., Zhang, H. B., Farook, U., Edirisinghe, M., Stride, E. & Colombo, P. 2008 Generation of multilayered structures for biomedical applications using a novel tri-needle coaxial device and electrohydrodynamic flow. *J. R. Soc. Interface* **5**, 1255–1261. (doi:10.1098/rsif.2008.0247)
15 Subramaniam, A. B., Abkarian, M., Mahadevan, L. & Stone, H. A. 2005 Colloid science: non-spherical bubbles. *Nature* **438**, 930. (doi:10.1038/438930a)
16 Boys, C. V. 1959 *Soap bubbles.* New York, NY: Dover.
17 Stride, E. & Edirisinghe, M. 2008 Novel microbubble preparation technologies. *Soft Matter* **4**, 2350–2359. (doi:10.1039/B809517P)
18 Hettiarachchi, K., Talu, E., Longo, M. L., Dayton, P. A. & Lee, A. P. 2007 On-chip generation of microbubbles as a practical technology for manufacturing contrast agents for ultrasonic imaging. *Lab Chip* **7**, 463–468. (doi:10.1039/b701481n)
19 Lee, M. H., Prasad, V. & Lee, D. 2010 Microfluidic fabrication of stable nanoparticle-shelled bubbles. *Langmuir* **26**, 2227–2230. (doi:10.1021/la904425v)
20 Xu, Q., Hashimoto, M., Dang, T. T., Hoare, T., Kohane, D. S., Whitesides, G. M., Langer, R. & Anderson, D. G. 2009 Preparation of monodisperse biodegradable polymer microparticles using a microfluidic flow-focusing device for controlled drug delivery. *Small* **5**, 1575–1581. (doi:10.1002/smll.200801855)
21 Luo, C. J., Nangrejo, M. & Edirisinghe, M. 2010 A novel method of selecting solvents for polymer electrospinning. *Polymer* **51**, 1654–1662. (doi:10.1016/j.polymer.2010.01.031)
22 da Silveira, R., Chaieb, S. & Mahadevan, L. 2000 Rippling instability of a collapsing bubble. *Science* **287**, 1468–1471. (doi:10.1126/science.287.5457.1468)
23 Garrett, W. D. 1981 Comment on 'Organic particle and aggregate formation resulting from the dissolution of bubbles in seawater'. *Limnol. Oceanogr.* **26**, 989–992. (doi:10.4319/lo.1981.26.5.0989)